

# Opioid Modulation of Ventral Pallidal Afferents to Ventral Tegmental Area Neurons

Gregory O. Hjelmstad, Yanfang Xia, Elyssa B. Margolis, and Howard L. Fields

Ernest Gallo Clinic and Research Center, Wheeler Center for the Neurobiology of Addiction, and Department of Neurology, University of California, San Francisco, Emeryville, California 94608

Activation of mu opioid receptors within the ventral tegmental area (VTA) can produce reward through the inhibition of GABAergic inputs. GABAergic neurons in the ventral pallidum (VP) provide a major input to VTA neurons. To determine the specific VTA neuronal targets of VP afferents and their sensitivity to mu opioid receptor agonists, we virally expressed channel rhodopsin (ChR2) in rat VP neurons and optogenetically activated their terminals in the VTA. Light activation of VP neuron terminals elicited GABAergic IPSCs in both dopamine (DA) and non-DA VTA neurons, and these IPSCs were inhibited by the mu opioid receptor agonist DAMGO. In addition, using a fluorescent retrograde marker to identify VTA-projecting VP neurons, we found them to be hyperpolarized by DAMGO. Both of these actions decrease GABAergic input onto VTA neurons, revealing two mechanisms by which endogenous or exogenous opioids can activate VTA neurons, including DA neurons.

## Introduction

Neurons within the ventral tegmental area (VTA) control the motivational and rewarding actions of palatable food and drugs of abuse (Wise, 1996; Everitt and Robbins, 2005; Fields et al., 2007; Berridge, 2009). Mu opioid receptors (MORs) within the VTA play a critical role in these behaviors. For example, MOR agonists are self-administered directly into the VTA (Bozarth and Wise, 1981; Devine and Wise, 1994) and, when microinjected into the VTA, produce conditioned place preference (Phillips and LePiane, 1980; Bals-Kubik et al., 1993), increase feeding (Jenck et al., 1986; Mucha and Iversen, 1986) and food seeking (Kelley et al., 1989), and reinstate drug seeking (Stewart, 1984). MOR antagonists injected into the VTA decrease consumption of ethanol (Margolis et al., 2008) and palatable food (Lamonte et al., 2002), GABA<sub>B</sub>-receptor-agonist-induced feeding (Khaimova et al., 2004), and cocaine conditioned place preference (Soderman and Unterwald, 2008). VTA opioids have been proposed to produce their reinforcing effects through the disinhibition of VTA dopamine (DA) neurons (Johnson and North, 1992). In fact, inhibitory control of midbrain DA neurons can robustly control behavior. For example, microinjection of a GABA<sub>A</sub> receptor antagonist into the VTA increases locomotor activity, and this is antagonized by a systemic DA receptor antagonist (Mogenson et al., 1979). Likewise, intra-VTA GABA<sub>A</sub> receptor antagonists pro-

duce conditioned place preference (Laviolette and van der Kooy, 2004; Laviolette et al., 2004), which can be blocked by intranucleus accumbens (NAc) DA antagonists in opioid-dependent animals (Laviolette et al., 2004). Finally, animals will self-administer GABA<sub>A</sub> receptor antagonists directly into the VTA (David et al., 1997; Ikemoto et al., 1997). Until recently, the most widely accepted model to explain these data was that a population of VTA GABAergic interneurons tonically inhibits VTA DA neurons and that reducing this inhibition activates DA neurons (Johnson and North, 1992; van Zessen et al., 2012). However, VTA DA neurons also receive dense GABAergic inputs from extrinsic sources and opioid control of these extrinsically derived inputs also robustly controls VTA DA neuron firing (see below).

A number of sources of GABA from extrinsic sites have been identified, including the NAc (Nauta et al., 1978), ventral pallidum (VP; Haber et al., 1985), rostromedial tegmental nucleus (RMTg) (Jhou et al., 2009) and pedunculopontine tegmental nucleus/lateral dorsal tegmentum (Omelchenko and Sesack, 2005; Good and Lupica, 2009). GABA release from afferents arising from both the NAc shell (Xia et al., 2011) and the RMTg (Matsui and Williams, 2011) is inhibited by MORs. Although GABAergic inputs from the RMTg clearly target DA neurons in both the VTA and neighboring substantia nigra (Balcita-Pedicino et al., 2011; Matsui and Williams, 2011), we reported previously that NAc inputs preferentially target non-DA neurons in the VTA (Xia et al., 2011). In contrast, neither the cellular connectivity of VP inputs to the VTA nor their opioid sensitivity has been determined. Given that activation of the VP produces reward (Tindell et al., 2004; Smith et al., 2009), understanding this connectivity is critical for interpreting how VP afferents control activity in the VTA. This is particularly important because there is evidence that the VP is a significant source of endogenous opioids for the VTA (Kalivas et al., 1993). Therefore, the VP neurons may inhibit

Received Jan. 10, 2013; revised March 4, 2013; accepted March 7, 2013.

Author contributions: G.O.H., E.B.M., and H.L.F. designed research; G.O.H. and Y.X. performed research; G.O.H. and Y.X. analyzed data; G.O.H., E.B.M., and H.L.F. wrote the paper.

This work was supported by the National Institutes of Health (Grant #R01 DA029776 to G.O.H.), the State of California for medical research on alcohol and substance abuse through the University of California, San Francisco, and the Wheeler Center for the Neurobiology of Addiction. We thank Chichen Qiu for technical assistance.

The authors declare no competing financial interests.

Correspondence should be addressed to Gregory Hjelmstad, Ernest Gallo Clinic and Research Center, 5858 Horton Street, Suite #200, Emeryville, CA 94608. E-mail: gregh@gallo.ucsf.edu.

DOI:10.1523/JNEUROSCI.0178-13.2013

Copyright © 2013 the authors 0270-6474/13/336454-06\$15.00/0

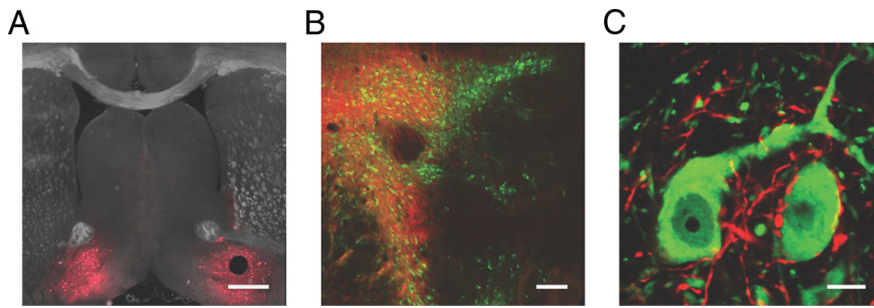


**Figure 1.** Ventral pallidal projections to the VTA. *A*, Coronal section showing bilateral expression of Chr2 (red) at the injection site in the VP. Scale bar, 500  $\mu$ m. *B*, Horizontal midbrain section showing Chr2-expressing VP fibers (red) projecting widely throughout the VTA and medial substantia nigra (TH immunocytochemical labeling shown in green). Scale bar, 200  $\mu$ m. *C*, High-magnification section in the VTA showing Chr2-expressing axons (red) contacting DA neuron cell bodies (green). Scale bar, 10  $\mu$ m.

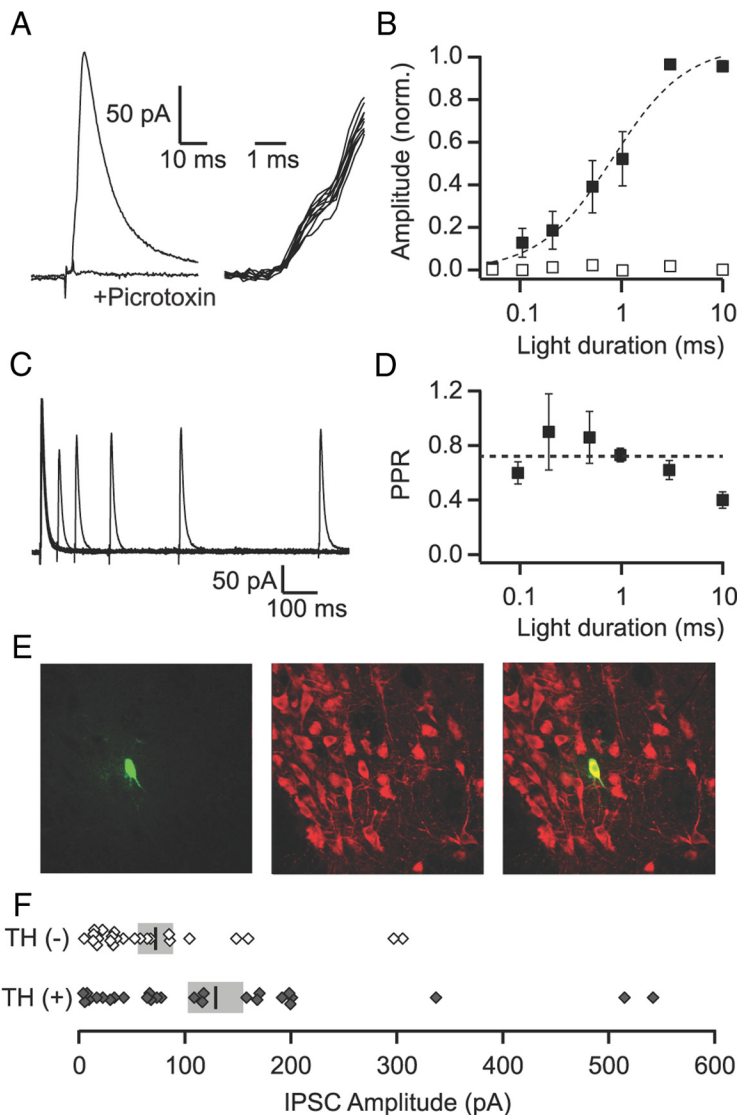


**Figure 2.** VP inputs produce GABA<sub>A</sub>-mediated IPSCs onto VTA neurons. *A*, Left: Average of 10 consecutive light-evoked IPSCs recorded under control conditions and in the presence of picrotoxin (100  $\mu$ M). Right: The individual IPSCs from the average shown on an expanded time scale (with the stimulus artifact subtracted out) indicate little trial-to-trial jitter in the onset of the current, which is consistent with a direct, monosynaptic input. *B*, IPSC amplitude as a function of light duration in control conditions (filled squares,  $n = 7$ ) and in the presence of TTX (1  $\mu$ M; open squares,  $n = 4$ ). *C*, Overlay of averages (5 sweeps each) of pairs of light-evoked IPSCs at intervals of 50, 100, 200, 400, and 800 ms from an example recording. *D*, The PPR (50 ms interspike interval) plotted as a function of the light duration. The dashed line is the average of across all durations. *E*, Example of a TH(+) neuron that showed a light-evoked response from the VP. Left: Biocytin fill (green); middle: TH (red); right: overlay. *F*, Distribution of evoked IPSC amplitudes for all identified TH(+) and TH(−) neurons. Vertical bars show mean amplitude for each group. SEM is shown in gray.

some VTA neurons directly via the release of GABA while disinhibiting others through the inhibitory actions of enkephalin at GABAergic terminals.

In the present study, we examined the synaptic physiology and connectivity of VP neuronal terminals in the VTA using a combination of electrophysiology, immunocytochemistry, and optogenetics. We found that VP neurons target both DA and non-DA neurons within the VTA and are inhibited by MOR activation both at their terminals and at their cell bodies.

## Materials and Methods

**Animals.** Surgeries were performed on 70–100 g male Sprague Dawley rats. Animals were anesthetized with isoflurane. In a subset of animals, AAV2/1-CAG-ChR2-tdtomato was bilaterally injected (500 nl in each side) using a Hamilton syringe stereotactically placed into the VP (AP, +1.0 mm from bregma; ML,  $\pm$ 1.7 mm from bregma; V, −7.7 mm from skull surface). The injector was left in place for 5 min, raised 1 mm, and left for an additional 5 min before slowly being completely removed. Animals were then returned to their home cages for 14–24 d before electrophysiological experiments were performed. For retrograde tracer experiments, neuro-DiI (1  $\mu$ l, 7% in ethanol; Biotium) or Fluorogold (1  $\mu$ l) was slowly injected (over 5 min) into the VTA (AP, −4.7; ML,  $\pm$ 0.8; DV, −8.1).

**Slice preparation and electrophysiology.** Horizontal midbrain slices including the VTA (150–200  $\mu$ m thick) or coronal VP slices (200  $\mu$ m thick) were prepared using a Vibratome (Leica Instruments) in artificial CSF (ACSF) containing the following (in mM): 119 NaCl, 2.5 KCl, 1.3 MgSO<sub>4</sub>, 1.0 NaH<sub>2</sub>PO<sub>4</sub>, 2.5 CaCl<sub>2</sub>, 26.2 NaHCO<sub>3</sub>, and 11 glucose (saturated with 95% O<sub>2</sub>/5% CO<sub>2</sub>). Slices were submerged in ACSF and allowed to recover for >1 h at room temperature before electrophysiological recordings.

Individual slices were visualized under an upright microscope (Olympus) with differential interference contrast optics and infrared and epifluorescent illumination. Whole-cell recordings were made with 2.5–4 M $\Omega$  pipettes containing the following (in mM): 123 K-gluconate, 10 HEPES, 0.2 EGTA, 8 NaCl, 2 MgATP, 0.3 Na<sub>3</sub>GTP, and 0.1% biocytin, pH 7.2, osmolarity adjusted to 275–285. Recordings were made using a Multiclamp 700A or 700B amplifier (Molecular Devices), filtered at 2 kHz, and collected at 5 kHz using procedures written for Igor Pro (Wavemetrics).

ChR2 was activated by transmitting 470 nm light (50  $\mu$ s to 10 ms) through the light path of the microscope using an LED (XR-E XLamp LED; Cree) powered by an LED driver (Mightex Systems). ChR2-evoked GABAergic IPSC amplitudes were calculated by comparing a 2 ms period at the peak of the response with a baseline just before light stimulation. Series resistance was monitored online by measuring

the peak of the capacitance transient in response to a 4 mV hyperpolarizing voltage step applied at the end of each sweep. All drugs were applied by bath perfusion. Stock solutions of drugs were made and diluted (typically 1 in 1000) into ACSF immediately before application. Liquid junction potential (calculated at 15 mV) has been corrected for.

Statistical analyses were performed using the Student's *t* test or appropriate statistic as described in the text. Data are presented as mean  $\pm$  SEM. Significance is defined as  $p < 0.05$ .

**Immunocytochemistry.** For determining tyrosine hydroxylase (TH) immunoreactivity, immediately after recording, slices were fixed in 4% formaldehyde for 2 h and then washed thoroughly and stored at 4°C in PBS. Sections were preblocked for 2 h in PBS plus 0.3% (v/v) Tween, 0.2% BSA, and 5% normal goat serum, and then incubated for 48 h at 4°C with a rabbit anti-TH polyclonal antibody (1:100). The slices were washed thoroughly in PBS with 0.3% Tween and 0.2% (w/v) BSA before being agitated overnight at 4°C with Cy5 anti-rabbit secondary antibody (1:100) and fluorescein-conjugated streptavidin (3.25  $\mu$ l/ml). Sections were mounted on slides using Bio-Rad Fluoroguard Antifade Reagent mounting media and visualized under a Zeiss LSM 510 META microscope. Neurons were categorized as TH(–) if they were in the same focal plane as other TH(+) neurons but contained no antibody labeling.

Tissue containing the injection sites was fixed in 4% formaldehyde and coronal sections (50  $\mu$ m) were prepared using a sliding microtome. Slices were preblocked in 10% normal goat serum for 30 min and then incubated with a rabbit anti-RFP antibody (1:2000) for 48 h. Slices were washed thoroughly before being incubated with FITC-conjugated affinity-pure goat anti-rabbit secondary antibody (1:200).

## Results

Microinjection of adeno-associated virus containing ChR2-tdtomato into the VP resulted in expression of ChR2 in VP cell bodies and their terminal fields in the VTA and laterally in the neighboring substantia nigra (Fig. 1*A, B*). In horizontal midbrain slices containing the VTA, we found strong fluorescence in fibers but not in cell bodies (Fig. 1*B*), which is consistent with axonal transport of ChR2 to the terminal fields of VP neurons. When costained with an antibody against TH, we often observed fluorescent fibers apposing and sometimes appearing to encapsulate TH(+) neurons (Fig. 1*C*), a phenomenon that we did not observe after microinjection of ChR2 into the NAc (Xia et al., 2011).

To investigate the functional connectivity of VP afferents within the VTA, we cut horizontal brain slices and made whole-cell voltage-clamp recordings from VTA neurons. Optical stimulation of VP fibers produced monosynaptic IPSCs that were blocked by the GABA<sub>A</sub> antagonist picrotoxin ( $98.5 \pm 2.8\%$ ,  $n = 17$ ; Fig. 2*A*). The amplitude of the light-evoked IPSC was dependent upon the intensity and duration of the light stimulus. Light pulses ranging in duration from 100  $\mu$ s to 10 ms produced an input/output curve with a half-maximum of 0.8 ms (Fig. 2*B*).

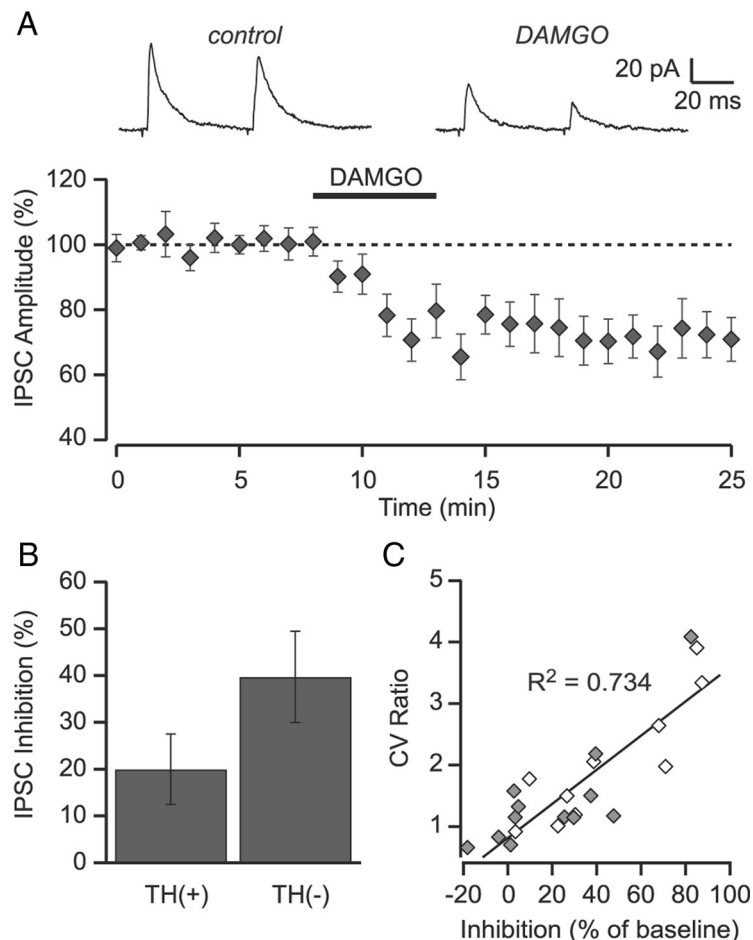


**Figure 3.** DAMGO inhibits light-evoked IPSCs. **A**, Bath application of the MOR agonist DAMGO (1  $\mu$ M) inhibited light-evoked IPSCs arising from the NAc ( $n = 23$ ). Inset shows average of 10 consecutive sweeps under control conditions and in DAMGO from a representative experiment. **B**, The magnitude of the DAMGO-mediated inhibition onto TH(+) ( $n = 13$ ) tended to be smaller than onto TH(–) ( $n = 10$ ) neurons. **C**, The change in the coefficient of variance following application of DAMGO is correlated with the degree of inhibition. Scatter plot of the amount of inhibition versus the change in the coefficient of variance for each individual cell. Filled symbols are TH(+); open symbols are TH(–). Solid line is the linear regression through all of the data ( $R^2 = 0.74$ ;  $p < 0.001$ ).

Moreover, consistent with previous observations (Cruikshank et al., 2010; Xia et al., 2011), light-evoked responses were completely blocked by the Na<sup>+</sup>-channel blocker tetrodotoxin (1  $\mu$ M; Fig. 2*B*), indicating that, like electrical stimulation, light-activated ChR2 evokes action potentials in nerve fibers, leading to the subsequent release of neurotransmitter.

Paired light stimuli produced paired pulse depression that was dependent upon the interstimulus interval (Fig. 2*C*). The paired pulse ratio (PPR) measured at a 50 ms interval averaged  $0.57 \pm 0.02$  ( $n = 40$ ). Despite the fact that our neurotransmitter release is action-potential dependent, it is possible that the PPR observed when using ChR2 is not reflective of the true PPR at the synapse, because the PPR is sensitive to residual calcium in the nerve terminal and ChR2 activates a nonselective cation current that has some permeability to calcium. To investigate this, we measured the PPR for different light stimulus durations: longer durations should increase residual calcium through the ChR2 channel and thus might influence the PPR. However, we found that the PPR was not influenced by the stimulus duration except for the longest (10 ms) duration (Fig. 2*D*). It remains unclear whether the increased depression at this duration is due to a change in short-term plasticity or to a decrease in the

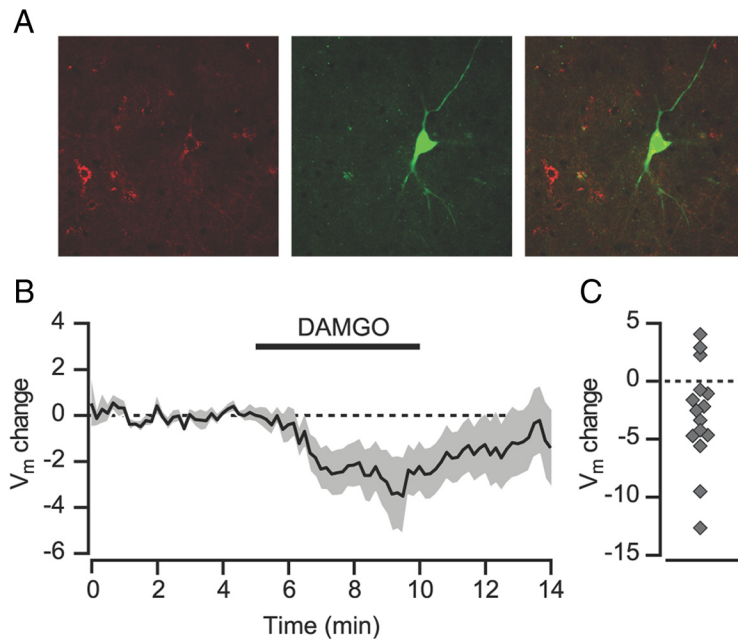


**Figure 4.** VP neurons retrogradely labeled from the VTA are hyperpolarized by mu opioids. **A**, Example of a Dil-filled VP neuron. Left: Dil (red); middle: biocytin fill (green); right: overlay. **B**, The membrane potential for VP neurons ( $n = 15$ ) was hyperpolarized after bath application of the MOR-selective agonist DAMGO ( $1 \mu\text{M}$ ). **C**, Scatter plot showing membrane potential change for each individual experiment.

ability of the second stimulus to reliably produce an action potential in the nerve fiber.

In our previous study investigating VTA inputs arising from the NAc, we found synaptic input only onto TH(−) (i.e., non-DA, VTA neurons; Xia et al., 2011). To confirm the apparent direct connection of VP inputs to VTA DA neurons we observed anatomically, we included biocytin in our microelectrode recording solution and, after recordings, processed the tissue for TH immunoreactivity (Fig. 2E). Of 52 processed neurons that showed a light-evoked input from the VP, 28 were TH(+). Therefore, VP inputs target both TH(+) and TH(−) neurons within the VTA. The mean amplitude of the IPSCs onto confirmed TH(+) neurons was larger than onto TH(−) neurons ( $128.9 \pm 26.2$  pA vs  $72.3 \pm 16.6$  pA; Fig. 2F). However, this was highly variable, plausibly due to differing levels of ChR2 expression across slices and/or animals. Nonetheless, a significantly larger proportion of neurons with light-evoked IPSCs larger than the median were TH(+) (18 of 26,  $p < 0.05$ , Pearson's  $\chi^2$  test).

Because MOR agonists' ability to inhibit GABA release onto VTA DA neurons is implicated in reward, and the VP inputs synapse onto DA neurons, we investigated whether these inputs were inhibited by MOR activation. In neurons in which we observed light-evoked IPSCs, we bath-applied the selective MOR agonist DAMGO ( $1 \mu\text{M}$ ). DAMGO significantly inhibited light-evoked GABA<sub>A</sub> IPSCs onto both TH(+) and TH(−) neurons ( $30.5 \pm 6.4\%$ ,  $n = 23$ ,  $p < 0.001$ ; Fig. 3A). There was a trend for a larger inhibition onto TH(−) neurons compared with TH(+) neurons, although this did not reach significance ( $44.2 \pm 9.8\%$  vs  $20.0 \pm 7.5\%$ , respectively,  $p = 0.065$ ; Fig. 3B). The DAMGO inhibition was not associated with an increase in the PPR measured at 50 ms ( $0.70 \pm 0.07$  vs  $0.59 \pm 0.06$ , respectively), but was associated with a significant increase in the coefficient of variance of the IPSC ( $67 \pm 21\%$  increase,  $p < 0.01$ ), a measure that is inversely correlated with the probability of release (Del Castillo and Katz, 1954; Manabe et al., 1993). Moreover, this change in

coefficient of variance was correlated with the magnitude of the DAMGO inhibition ( $r^2 = 0.72$ ; Fig. 3C), implicating a presynaptic inhibition of GABA release.

VP neurons receive direct input from NAc GABAergic neurons that co-contain the endogenous opioid enkephalin (Lu et al., 1998). *In vivo*, approximately half of VP neurons are inhibited after local iontophoresis of DAMGO (Mitrovic and Napier, 1995), but it is unclear whether the opioid-sensitive VP neurons project to the VTA. To determine whether VTA-projecting VP neurons are inhibited directly by DAMGO, we retrogradely labeled VTA-projecting VP neurons by microinjecting either Dil or Fluorogold into the VTA. We then made whole-cell current-clamp recordings from fluorescing VP neurons (Fig. 4A) in coronal brain slices at the neuron's resting membrane potential ( $-56.7 \pm 2.4$  mV). Bath application of the MOR selective agonist DAMGO ( $1 \mu\text{M}$ ) produced a significant hyperpolarization in VTA-projecting VP neurons ( $-2.91 \pm 1.14$  mV,  $p < 0.05$ ,  $n = 15$ ; Fig. 4B, C). Therefore, mu opioids hyperpolarize many VTA-projecting VP neuronal somata directly and inhibit GABA release from VP terminals within the VTA.

## Discussion

This work extends our understanding of the circuitry underlying DA-mediated opioid reward. Disinhibition of VTA DA neurons can produce positive reinforcement, and the present study shows that opioids can influence the inhibition of VTA DA neurons by the VP through two separate mechanisms: inhibition of their somata in the VP and inhibition of their GABAergic terminals on VTA DA neurons.

The apparent direct GABAergic synaptic connection of VP terminals to VTA cell bodies parallels earlier observations that globus pallidus inputs onto DA neurons of the substantia nigra often form baskets around the soma and proximal dendrites of nigral cells (Smith and Bolam, 1990). Therefore, VP inputs are positioned to strongly inhibit cell bodies and thus influence the overall firing rate of midbrain neurons. Our findings also extend our understanding of an *in vivo* study showing that VP GABAergic inputs control the population activity of VTA DA neurons (Floresco et al., 2003).

Similar to inputs arising from the NAc (Xia et al., 2011) and from the RMTg (Matsui and Williams, 2011), VTA GABAergic terminals of VP neurons are sensitive to MOR activation. We observed a larger, opioid-mediated inhibition of VP IPSCs on confirmed TH(−) neurons compared with TH(+) neurons. However, this effect was highly variable in both groups: some TH(+) neurons showed large DAMGO-mediated inhibitions and some TH(−) neurons had IPSCs that were unaffected by DAMGO. This raises the possibility that opioids preferentially inhibit VP inputs onto specific subsets of VTA neurons, based either on neurotransmitter content (e.g., GABA vs glutamate) or projection target (e.g., NAc-projecting vs PFC-projecting). Likewise, endogenous opioid release from VP terminals could diffuse

within the VTA to inhibit neurotransmitter release from other GABAergic terminals such as those arising from the RMTg.

Like the VTA, the VP has also been implicated in the rewarding actions of both palatable food and drugs of abuse (Hubner and Koob, 1990; Bardo, 1998; McFarland and Kalivas, 2001; Tang et al., 2005; Mickiewicz et al., 2009; Smith et al., 2009). For example, lesions of the VP reduce operant responding for cocaine or alcohol (for review, see Smith et al., 2009). Moreover, opioids microinjected into the posterior VP enhance both the motivation to eat and hedonic responses to food (Smith and Berridge, 2007). Although which specific subpopulations of VP neurons are required to produce these behaviors is not yet clear, the presence of opioid receptors on VTA-projecting VP neurons raises the possibility that the direct connection from the VP to the VTA represents a specific node in a feeding circuit.

VP neurons project to a wide number of brain regions in addition to the VTA, including the medial dorsal thalamus, subthalamic nucleus, lateral hypothalamus, and the substantia nigra, as well as making reciprocal connections with the NAc (Haber et al., 1985; Zahm, 1989; Groenewegen et al., 1993; Tripathi et al., 2012). Based on cytoarchitecture, the VP can be divided into two subregions (Zahm and Heimer, 1988). Our infections typically spanned both subregions; however, the medial VP is the primary source of VTA afferents, whereas the lateral VP targets the substantia nigra (Zahm, 1989). Conversely, in a recent study, investigators traced single axons from VP neurons and reported that both medial and lateral VP neurons can target the VTA (Tripathi et al., 2012). Moreover, they observed that individual VP neurons targeted several brain regions and their projection patterns were highly variable. This variability is reflected in our finding that both DA and non-DA neurons in the VTA are targeted by the VP. It is unclear whether the targeted non-DA neurons are GABAergic or glutamatergic or both. Consistent with targeting VTA GABA neurons, the VP projects to the RMTg (Jhou et al., 2009; Kaufling et al., 2009), a group of GABAergic neurons that overlap with the caudal VTA and heavily innervate DA neurons in the VTA and substantia nigra pars compacta (Balcita-Pedicino et al., 2011). This potential indirect pathway (either through the RMTg or through local GABAergic interneurons) from the VP to VTA DA neurons would excite (disinhibit) DA neurons when activated, countering the direct inhibition of DA neurons by VP. Indeed, this indirect pathway provides a possible circuit explanation for how GABA<sub>A</sub> antagonists infused into VP increase both locomotion and DA metabolites in the NAc (Austin and Kalivas, 1991). It is also possible that the VP targets VTA glutamate neurons. Intriguingly, a subset of VTA glutamate neurons innervate the VP (Hnasko et al., 2012) raising the possibility of a reciprocal connection between neurons in these two regions.

In summary, VP neurons projecting to the VTA are part of a distributed MOR-sensitive network that exerts robust control over motivated behaviors. Further elucidation of the upstream and downstream elements of the circuit and determining the physiological conditions under which it is activated will greatly increase our understanding of the role of opioids in motivated behavior and positive reinforcement.

## References

- Austin MC, Kalivas PW (1991) Dopaminergic involvement in locomotion elicited from the ventral pallidum/substantia innominata. *Brain Res* 542:123–131. [CrossRef Medline](#)
- Balcita-Pedicino JJ, Omelchenko N, Bell R, Sesack SR (2011) The inhibitory influence of the lateral habenula on midbrain dopamine cells: ultrastructural evidence for indirect mediation via the rostromedial mesopontine tegmental nucleus. *J Comp Neurol* 519:1143–1164. [CrossRef Medline](#)
- Bals-Kubik R, Ableitner A, Herz A, Shippenberg TS (1993) Neuroanatomical sites mediating the motivational effects of opioids as mapped by the conditioned place preference paradigm in rats. *J Pharmacol Exp Ther* 264:489–495. [Medline](#)
- Bardo MT (1998) Neuropharmacological mechanisms of drug reward: beyond dopamine in the nucleus accumbens. *Crit Rev Neurobiol* 12:37–67. [CrossRef Medline](#)
- Berridge KC (2009) 'Liking' and 'wanting' food rewards: brain substrates and roles in eating disorders. *Physiol Behav* 97:537–550. [CrossRef Medline](#)
- Bozarth MA, Wise RA (1981) Intracranial self-administration of morphine into the ventral tegmental area in rats. *Life Sci* 28:551–555. [CrossRef Medline](#)
- Cruikshank SJ, Urabe H, Nurmikko AV, Connors BW (2010) Pathway-specific feedforward circuits between thalamus and neocortex revealed by selective optical stimulation of axons. *Neuron* 65:230–245. [CrossRef Medline](#)
- David V, Durkin TP, Cazala P (1997) Self-administration of the GABA<sub>A</sub> antagonist bicuculline into the ventral tegmental area in mice: dependence on D2 dopaminergic mechanisms. *Psychopharmacology (Berl)* 130:85–90. [CrossRef Medline](#)
- Del Castillo J, Katz B (1954) Quantal components of the end-plate potential. *J Physiol* 124:560–573. [Medline](#)
- Devine DP, Wise RA (1994) Self-administration of morphine, DAMGO, and DPDPE into the ventral tegmental area of rats. *J Neurosci* 14:1978–1984. [Medline](#)
- Everitt BJ, Robbins TW (2005) Neural systems of reinforcement for drug addiction: from actions to habits to compulsion. *Nat Neurosci* 8:1481–1489. [CrossRef Medline](#)
- Fields HL, Hjelmstad GO, Margolis EB, Nicola SM (2007) Ventral Tegmental Area Neurons in Learned Appetitive Behavior and Positive Reinforcement. *Annu Rev Neurosci* 30:289–316. [CrossRef Medline](#)
- Floresco SB, West AR, Ash B, Moore H, Grace AA (2003) Afferent modulation of dopamine neuron firing differentially regulates tonic and phasic dopamine transmission. *Nat Neurosci* 6:968–973. [CrossRef Medline](#)
- Good CH, Lupica CR (2009) Properties of distinct ventral tegmental area synapses activated via pedunculo-pontine or ventral tegmental area stimulation in vitro. *J Physiol* 587:1233–1247. [CrossRef Medline](#)
- Groenewegen HJ, Berendse HW, Haber SN (1993) Organization of the output of the ventral striatopallidal system in the rat: ventral pallidal efferents. *Neuroscience* 57:113–142. [CrossRef Medline](#)
- Haber SN, Groenewegen HJ, Grove EA, Nauta WJ (1985) Efferent connections of the ventral pallidum: evidence of a dual striato pallidofugal pathway. *J Comp Neurol* 235:322–335. [CrossRef Medline](#)
- Hnasko TS, Hjelmstad GO, Fields HL, Edwards RH (2012) Ventral tegmental area glutamate neurons: electrophysiological properties and projections. *J Neurosci* 32:15076–15085. [CrossRef Medline](#)
- Hubner CB, Koob GF (1990) The ventral pallidum plays a role in mediating cocaine and heroin self-administration in the rat. *Brain Res* 508:20–29. [CrossRef Medline](#)
- Ikemoto S, Murphy JM, McBride WJ (1997) Self-infusion of GABA(A) antagonists directly into the ventral tegmental area and adjacent regions. *Behav Neurosci* 111:369–380. [CrossRef Medline](#)
- Jenck F, Gratton A, Wise RA (1986) Opposite effects of ventral tegmental and periaqueductal gray morphine injections on lateral hypothalamic stimulation-induced feeding. *Brain Res* 399:24–32. [CrossRef Medline](#)
- Jhou TC, Geisler S, Marinelli M, Degarmo BA, Zahm DS (2009) The mesopontine rostromedial tegmental nucleus: A structure targeted by the lateral habenula that projects to the ventral tegmental area of Tsai and substantia nigra compacta. *J Comp Neurol* 513:566–596. [CrossRef Medline](#)
- Johnson SW, North RA (1992) Opioids excite dopamine neurons by hyperpolarization of local interneurons. *J Neurosci* 12:483–488. [Medline](#)
- Kalivas PW, Churchill L, Klitenick MA (1993) GABA and enkephalin projection from the nucleus accumbens and ventral pallidum to the ventral tegmental area. *Neuroscience* 57:1047–1060. [CrossRef Medline](#)
- Kaufling J, Veinante P, Pawlowski SA, Freund-Mercier MJ, Barrot M (2009) Afferents to the GABAergic tail of the ventral tegmental area in the rat. *J Comp Neurol* 513:597–621. [CrossRef Medline](#)
- Kelley AE, Cadore M, Stinus L, Le Moal M (1989) Neurotensin, substance P, neurokinin-alpha, and enkephalin: injection into ventral tegmental area

- in the rat produces differential effects on operant responding. *Psychopharmacology (Berl)* 97:243–252. [CrossRef Medline](#)
- Khaimova E, Kandov Y, Israel Y, Cataldo G, Hadjimarkou MM, Bodnar RJ (2004) Opioid receptor subtype antagonists differentially alter GABA agonist-induced feeding elicited from either the nucleus accumbens shell or ventral tegmental area regions in rats. *Brain Res* 1026:284–294. [CrossRef Medline](#)
- Lamonte N, Echo JA, Ackerman TF, Christian G, Bodnar RJ (2002) Analysis of opioid receptor subtype antagonist effects upon mu opioid agonist-induced feeding elicited from the ventral tegmental area of rats. *Brain Res* 929:96–100. [CrossRef Medline](#)
- Laviolette SR, van der Kooy D (2004) GABA receptors signal bidirectional reward transmission from the ventral tegmental area to the tegmental pedunculopontine nucleus as a function of opiate state. *Eur J Neurosci* 20:2179–2187. [CrossRef Medline](#)
- Laviolette SR, Gallegos RA, Henriksen SJ, van der Kooy D (2004) Opiate state controls bi-directional reward signaling via GABA receptors in the ventral tegmental area. *Nat Neurosci* 7:160–169. [CrossRef Medline](#)
- Lu XY, Ghasemzadeh MB, Kalivas PW (1998) Expression of D1 receptor, D2 receptor, substance P and enkephalin messenger RNAs in the neurons projecting from the nucleus accumbens. *Neuroscience* 82:767–780. [Medline](#)
- Manabe T, Wyllie DJ, Perkel DJ, Nicoll RA (1993) Modulation of synaptic transmission and long-term potentiation: effects on paired pulse facilitation and EPSC variance in the CA1 region of the hippocampus. *J Neurophysiol* 70:1451–1459. [Medline](#)
- Margolis EB, Fields HL, Hjelmstad GO, Mitchell JM (2008) Delta-opioid receptor expression in the ventral tegmental area protects against elevated alcohol consumption. *J Neurosci* 28:12672–12681. [CrossRef Medline](#)
- Matsui A, Williams JT (2011) Opioid-sensitive GABA inputs from rostromedial tegmental nucleus synapse onto midbrain dopamine neurons. *J Neurosci* 31:17729–17735. [CrossRef Medline](#)
- McFarland K, Kalivas PW (2001) The circuitry mediating cocaine-induced reinstatement of drug-seeking behavior. *J Neurosci* 21:8655–8663. [Medline](#)
- Mickiewicz AL, Dallimore JE, Napier TC (2009) The ventral pallidum is critically involved in the development and expression of morphine-induced sensitization. *Neuropsychopharmacology* 34:874–886. [CrossRef Medline](#)
- Mitrovic I, Napier TC (1995) Electrophysiological demonstration of mu, delta and kappa opioid receptors in the ventral pallidum. *J Pharmacol Exp Ther* 272:1260–1270. [Medline](#)
- Mogenson GJ, Wu M, Manchanda SK (1979) Locomotor activity initiated by microinfusions of picrotoxin into the ventral tegmental area. *Brain Res* 161:311–319. [CrossRef Medline](#)
- Mucha RF, Iversen SD (1986) Increased food intake after opioid microinjections into nucleus accumbens and ventral tegmental area of rat. *Brain Res* 397:214–224. [CrossRef Medline](#)
- Nauta WJ, Smith GP, Faull RL, Domesick VB (1978) Efferent connections and nigral afferents of the nucleus accumbens septi in the rat. *Neuroscience* 3:385–401. [CrossRef Medline](#)
- Omelchenko N, Sesack SR (2005) Laterodorsal tegmental projections to identified cell populations in the rat ventral tegmental area. *J Comp Neurol* 483:217–235. [CrossRef Medline](#)
- Phillips AG, LePiane FG (1980) Reinforcing effects of morphine microinjection into the ventral tegmental area. *Pharmacol Biochem Behav* 12:965–968. [CrossRef Medline](#)
- Smith KS, Berridge KC (2007) Opioid limbic circuit for reward: interaction between hedonic hotspots of nucleus accumbens and ventral pallidum. *J Neurosci* 27:1594–1605. [CrossRef Medline](#)
- Smith KS, Tindell AJ, Aldridge JW, Berridge KC (2009) Ventral pallidum roles in reward and motivation. *Behav Brain Res* 196:155–167. [CrossRef Medline](#)
- Smith Y, Bolam JP (1990) The output neurones and the dopaminergic neurones of the substantia nigra receive a GABA-containing input from the globus pallidus in the rat. *J Comp Neurol* 296:47–64. [CrossRef Medline](#)
- Soderman AR, Unterwald EM (2008) Cocaine reward and hyperactivity in the rat: sites of mu opioid receptor modulation. *Neuroscience* 154:1506–1516. [CrossRef Medline](#)
- Stewart J (1984) Reinstatement of heroin and cocaine self-administration behavior in the rat by intracerebral application of morphine in the ventral tegmental area. *Pharmacol Biochem Behav* 20:917–923. [CrossRef Medline](#)
- Tang XC, McFarland K, Cagle S, Kalivas PW (2005) Cocaine-induced reinstatement requires endogenous stimulation of mu-opioid receptors in the ventral pallidum. *J Neurosci* 25:4512–4520. [CrossRef Medline](#)
- Tindell AJ, Berridge KC, Aldridge JW (2004) Ventral pallidal representation of Pavlovian cues and reward: population and rate codes. *J Neurosci* 24:1058–1069. [CrossRef Medline](#)
- Tripathi A, Prensa L, Mengual E (2012) Axonal branching patterns of ventral pallidal neurons in the rat. *Brain Struct Funct*.
- van Zessen R, Phillips JL, Budygin EA, Stuber GD (2012) Activation of VTA GABA neurons disrupts reward consumption. *Neuron* 73:1184–1194. [CrossRef Medline](#)
- Wise RA (1996) Neurobiology of addiction. *Curr Opin Neurobiol* 6:243–251. [CrossRef Medline](#)
- Xia Y, Driscoll JR, Wilbrecht L, Margolis EB, Fields HL, Hjelmstad GO (2011) Nucleus Accumbens Medium Spiny Neurons Target Non-Dopaminergic Neurons in the Ventral Tegmental Area. *J Neurosci* 31:7811–7816. [CrossRef Medline](#)
- Zahm DS (1989) The ventral striatopallidal parts of the basal ganglia in the rat—II. Compartmentation of ventral pallidal efferents. *Neuroscience* 30:33–50. [CrossRef Medline](#)
- Zahm DS, Heimer L (1988) Ventral striatopallidal parts of the basal ganglia in the rat: I. Neurochemical compartmentation as reflected by the distributions of neurotensin and substance P immunoreactivity. *J Comp Neurol* 272:516–535. [CrossRef Medline](#)